

Nucleolar protein B23/nucleophosmin regulates the vertebrate SUMO pathway through SENP3 and SENP5 proteases

Chawon Yun,¹ Yonggang Wang,¹ Debaditya Mukhopadhyay,¹ Peter Backlund,² Nagamalleswari Kolli,³ Alfred Yergey,² Keith D. Wilkinson,³ and Mary Dasso¹

¹Laboratory of Gene Regulation and Development, ²Section on Mass Spectrometry & Metabolism/Office of the Scientific Director, National Institute of Child Health and Human Development, Bethesda, MD 20892

³Department of Biochemistry, Emory University, Atlanta, GA 30322

Ubiquitin-like protein/sentrin-specific proteases (Ulp/SENPs) mediate both processing and deconjugation of small ubiquitin-like modifier proteins (SUMOs). Here, we show that Ulp/SENPs family members SENP3 and SENP5 localize within the granular component of the nucleolus, a subnucleolar compartment that contains B23/nucleophosmin. B23/nucleophosmin is an abundant shuttling phosphoprotein, which plays important roles in ribosome biogenesis and which has been strongly implicated in hematopoietic malignancies. Moreover, we found that B23/nucleophosmin binds SENP3

and SENP5 in *Xenopus laevis* egg extracts and that it is essential for stable accumulation of SENP3 and SENP5 in mammalian tissue culture cells. After either codepletion of SENP3 and SENP5 or depletion of B23/nucleophosmin, we observed accumulation of SUMO proteins within nucleoli. Finally, depletion of these Ulp/SENPs causes defects in ribosome biogenesis reminiscent of phenotypes observed in the absence of B23/nucleophosmin. Together, these results suggest that regulation of SUMO deconjugation may be a major facet of B23/nucleophosmin function in vivo.

Introduction

Small ubiquitin-like modifier proteins (SUMOs) are ubiquitin-related proteins that act in many processes through covalent linkage to cellular proteins (Johnson, 2004). Mammalian cells express three major SUMO paralogues: mature SUMO-2 and SUMO-3 are ~95% identical to each other and each is ~45% identical to SUMO-1. (Where they cannot be distinguished, SUMO-2 and -3 will be collectively called SUMO-2/3.) SUMO-1 localizes within the nucleoplasm, nuclear envelope, and nucleolus, whereas SUMO-2 and SUMO-3 are predominantly found in the nucleoplasm (Ayaydin and Dasso, 2004). All newly synthesized SUMOs are processed by ubiquitin-like protein/sentrin-specific proteases (Ulp/SENPs), and Ulp/SENPs also deconjugate SUMOylated species (Hay, 2007; Mukhopadhyay

and Dasso, 2007). *Saccharomyces cerevisiae* has two Ulp/SENPs, Ulp1p and Ulp2p (Li and Hochstrasser, 1999, 2000). Ulp1p is essential and localizes to nuclear pores, whereas Ulp2p is dispensable for growth and localizes to the nucleoplasm. Ulp1p has been particularly implicated in ribosome biogenesis (Panse et al., 2006).

The nucleolus is the site of ribosome synthesis, including preribosomal RNA transcription, ribosomal RNA (rRNA) processing, and ribosomal subunit assembly (Boisvert et al., 2007). B23/nucleophosmin is an abundant 37-kD phosphoprotein that shuttles between the granular component of the nucleolus and cytoplasm. B23/nucleophosmin can become SUMO conjugated under some circumstances (Liu et al., 2007). It has been implicated in many cellular processes, including ribosome biogenesis and export, centrosome duplication, and maintenance of genomic integrity through the Arf-MDM2-p53 pathway (Grisendi et al., 2006; Sherr, 2006). Consistent with these diverse roles,

C. Yun and Y. Wang contributed equally to this paper.

Correspondence to Mary Dasso: mdasso@helix.nih.gov

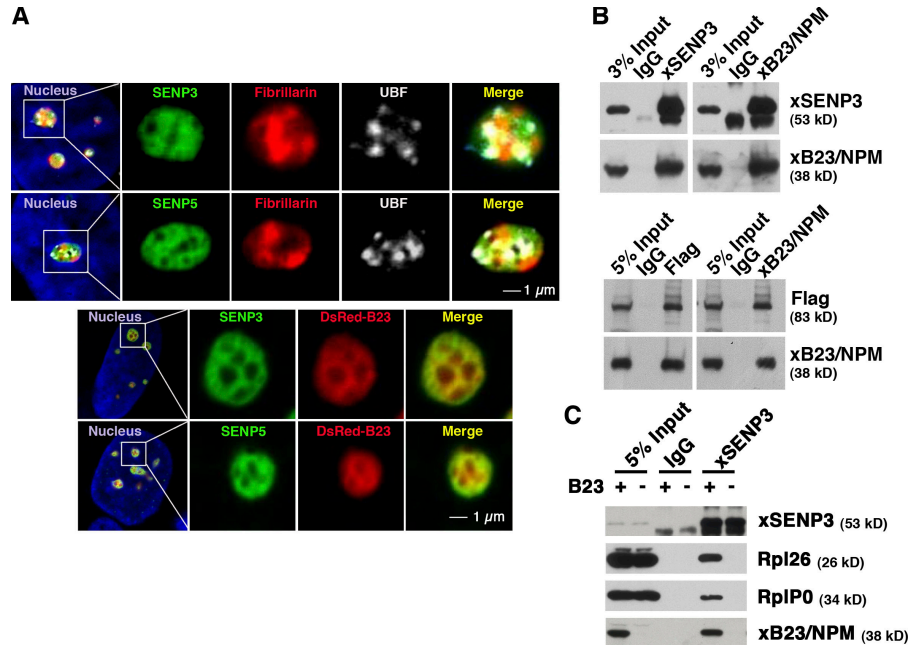
C. Yun's present address is Feinberg School of Medicine, Northwestern University, Chicago, IL 60611.

Abbreviations used in this paper: Ni-NTA, nickel-nitrilotriacetic acid; RNAi, RNA interference; rRNA, ribosomal RNA; SUMO, small ubiquitin-like modifier protein; Ulp/SENPs, ubiquitin-like protein/sentrin-specific protease; XEE, *Xenopus laevis* egg extract; xSENP3, *Xenopus* SENP3.

The online version of this article contains supplemental material.

This article is distributed under the terms of an Attribution-Noncommercial-Share Alike-No Mirror Sites license for the first six months after the publication date (see <http://www.jcb.org/misc/terms.shtml>). After six months it is available under a Creative Commons License (Attribution-Noncommercial-Share Alike 3.0 Unported license, as described at <http://creativecommons.org/licenses/by-nc-sa/3.0/>).

Figure 1. SENP3 and SENP5 colocalize and associate with B23/nucleophosmin. (A) U2OS-derived cell lines expressing GFP-SENP3 and GFP-SENP5 were transfected with a plasmid for expression of dsRed-fibrillarin (top). After 48 h, the cells were fixed and immunostained with monoclonal anti-UBF antibodies. The left column shows GFP, dsRed, and anti-UBF in the context of the nucleus, with DNA stained in blue using Hoechst 33342. The same cells were transfected with dsRed-B23/nucleophosmin (bottom). (B) Rabbit IgG (IgG), anti-xSENP3, or anti-xB23/nucleophosmin (xB23/NPM) antibodies were used for immunoprecipitation from 100 μ l of interphase XEE. The samples were subjected to SDS-PAGE and immunoblotting with anti-xSENP3 or anti-B23/nucleophosmin antibodies. To test xSENP5 binding to xB23/nucleophosmin, 25 μ l of XEE containing in vitro-translated FLAG-tagged xSENP5 was mixed with equal volume of interphase XEE. Immunoprecipitations were performed with anti-FLAG or anti-xB23/NPM antibodies (bottom). The samples were subjected to immunoblotting with anti-FLAG or anti-xB23/NPM antibodies. (C) Anti-xSENP3 was used for immunoprecipitation from IgG-treated control (+) or xB23/NPM-depleted (-) XEEs. The samples were subjected to SDS-PAGE and Western blotting with anti-xSENP3, -Rpl26, -RplP0, or -xB23/NPM antibodies, as indicated on the right.



B23/nucleophosmin binds to nucleic acids, nucleolar components, transcription factors, and histones, as well as to proteins involved in cell proliferation, mitosis, and oncogenic stress responses (Grisendi et al., 2006). It is not clear how these aspects of B23/nucleophosmin may be integrated with each other. Notably, B23/nucleophosmin is often overexpressed in solid tumors and has been strongly linked to hematopoietic malignancies (Grisendi et al., 2006).

We have examined the subnucleolar localization, behavior, and function of two nucleolar Ulp1p-like SUMO proteases, SENP3 and SENP5 (Di Bacco et al., 2006; Gong and Yeh, 2006; Mukhopadhyay and Dasso, 2007). We found that both of these enzymes colocalize and physically interact with B23/nucleophosmin. Moreover, B23/nucleophosmin is essential for their stable accumulation. After either codepletion of these Ulp/SENPs or depletion of B23/nucleophosmin, SUMO proteins accrue within nucleoli. Importantly, depletion of SENP3 and SENP5 causes defects in ribosome biogenesis reminiscent of those observed in the absence of B23/nucleophosmin. Collectively, our findings indicate that regulation of SUMO deconjugation through SENP3 and SENP5 may be a major facet of B23/nucleophosmin function and suggest that at least some of the diverse phenotypes found after disruption of B23/nucleophosmin can be attributed to defects of SUMOylation.

Results and discussion

We compared the localization of stably expressed GFP-SENP3 and GFP-SENP5 with components that are characteristic of nucleolar subcompartments, including the fibrillar centers (anti-UBF), the dense fibrillar component (dsRed-fibrillarin), and the

granular component (dsRed-B23/nucleophosmin). The signal from GFP-SENP3 and GFP-SENP5 overlapped poorly with UBF staining and only partially with dsRed-fibrillarin, suggesting that they were not concentrated in either the fibrillar centers or the dense fibrillar component (Fig. 1 A, top). In contrast, both proteins showed distributions that were very similar to B23/nucleophosmin, which could be observed either by immunostaining or by coexpression of B23/nucleophosmin as a fusion with the dsRed fluorescent protein (Fig. 1 A, bottom). We conclude that SENP3 and SENP5 are concentrated within the granular component.

The presence of SUMO-2/3-specific proteases within nucleoli suggested that the absence of these SUMO paralogues might be the result of their ongoing removal from nucleolar targets. To test this idea, we depleted SENP3 and SENP5 individually and together by oligonucleotide-mediated RNA interference (RNAi) from HeLa cells (Fig. 2 A). Depletion of either protease did not substantially alter the distribution of SUMO proteins. However, nucleolar SUMO-1 increased after codepletion of SENP3 and SENP5 (Fig. 2 B and Fig. S1, available at <http://www.jcb.org/cgi/content/full/jcb.200807185/DC1>). Significantly, SUMO-2/3 also became concentrated within nucleoli in the absence of both enzymes. The redistribution of SUMO-2/3 was striking because these paralogues are normally not evident within nucleoli. Depletion of nuclear pore-associated SENP/Ulps (SENP1 and SENP2) did not increase nucleolar levels of SUMO proteins (unpublished data), arguing that such accumulation is not a general result of SUMO pathway manipulation or of RNAi machinery activation.

SENP3 and SENP5 show robust enzymatic activities against SUMO-2/3-containing substrates (Di Bacco et al., 2006;

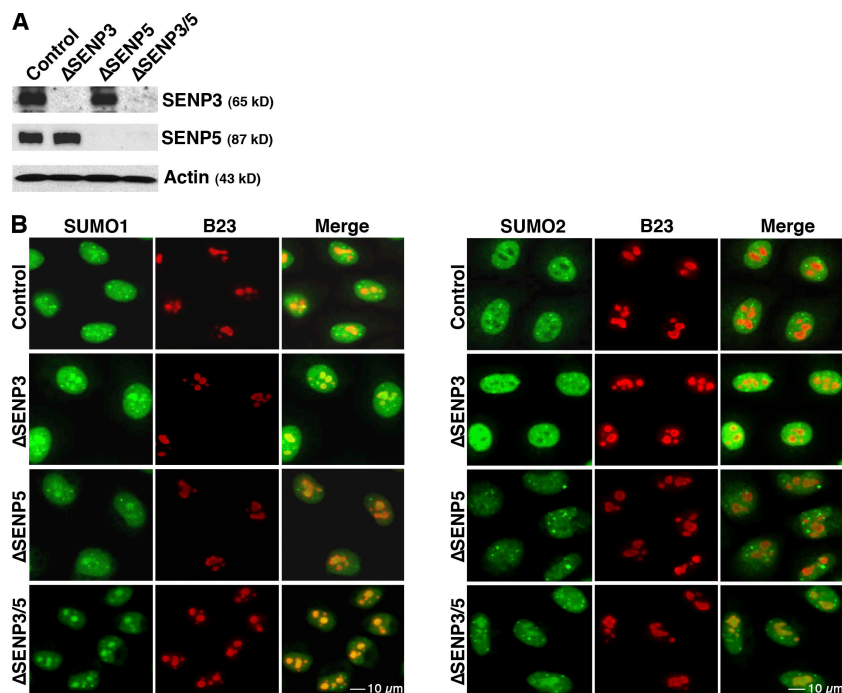


Figure 2. **SENP3 and SENP5 codepletion cause nucleolar SUMO protein accumulation.** (A) HeLa cells were transfected with siRNAs directed against SENP3 and SENP5, either singly or in combination. 72 h after transfection, depletion was confirmed by Western blotting. (B) Cells depleted of SENP3, SENP5, or both proteins were stained with antibodies against B23/nucleophosmin (B23; red) and either SUMO-1 (left; green) or SUMO-2/3 (right; green).

Gong and Yeh, 2006; Fig. S2, available at <http://www.jcb.org/cgi/content/full/jcb.200807185/DC1>), so they may directly control the half-lives of nucleolar SUMO-2/3-conjugated species. The functions of SENP3 and SENP5 appear to be at least partially redundant because high levels of SUMO-2/3 did not accumulate unless both proteins were depleted. Their role in controlling nucleolar SUMO-1 accumulation is somewhat harder to understand. It is possible that deconjugation of multiple SUMO moieties from some targets must occur in a particular sequence, so that failure to remove SUMO-2/3 in the absence of SENP3 and SENP5 might block subsequent removal of SUMO-1, and thus indirectly result in its nucleolar accumulation. Alternatively, SENP3 and SENP5 may be more active in vivo against SUMO-1-conjugated species than indicated by in vitro assays.

Budding yeast Ulp1p is required for 60S preribosome maturation and export (Panse et al., 2006). To test whether SENP3 and SENP5 are similarly required, we examined rRNA synthesis and processing through pulse-chase analysis with [³H]uridine (Fig. 3). Although 47S rRNA transcription was not substantially decreased after SENP3 depletion, the production of 28S rRNA from their 32S precursor RNA was inhibited. After a 2-h chase, control cells showed a ratio of labeled 32S versus 28S RNAs that was less than 0.5:1, whereas this ratio was over 2:1 in SENP3-depleted cells (Fig. 3 B). In contrast, loss of SENP5 did not have a strong effect on rRNA processing, but caused the levels of 47S RNA transcription to drop by >60% (Fig. 3 C). Cells depleted of both proteins showed both decreased 47S RNA precursor levels and increased 32S/28S ratios. Relocalization of ribosomal assembly factors further suggested disruption of ribosome biogenesis in the absence of SENP3 and SENP5 (Fig. S3, available at <http://www.jcb.org/cgi/content/full/jcb.200807185/DC1>). Simultaneous depletion of SENP1 and SENP2 marginally reduced 47S RNA transcription but did not appreciably alter the rate of rRNA processing or alter assembly factor localization (unpublished data), arguing

that defects in ribosome biogenesis were specifically caused by depletion of SENP3 and SENP5. Our results show that SENP3 and SENP5 individually play important roles in ribosome biogenesis (Fig. 3), but depletion of both proteases is required for elevation of SUMO-conjugated species within nucleoli (Fig. 2). Together, these results might suggest that although both SENP3 and SENP5 can act on the bulk of nucleolar substrates, they may each specifically regulate a subset of conjugates that are critical for particular events in the biogenesis pathway.

We were unable to extract SENP3 and SENP5 from mammalian nucleoli under conditions that would allow analysis of protein-protein interactions. As an alternative, we used *Xenopus laevis* egg extracts (XEEs) to look for binding partners. XEEs offer major advantages for these experiments because most nuclear and nucleolar proteins are stored in soluble forms (Powers et al., 2001). Human SENP3 and *Xenopus* SENP3 (xSENP3) proteins are ~85% identical within their catalytic domains and 50% identical throughout their entire sequences. Human SENP5 and xSENP5 proteins are ~87% identical within their catalytic domains and 43% identical throughout their entire sequences. There was little xSENP5 in *Xenopus* eggs (unpublished data), which is perhaps consistent with the more specialized tissue distribution of mammalian SENP5 (Fig. S2 C). Antibodies against xSENP3 recognized a protein of the appropriate size in XEEs. Analysis using vinyl sulfone derivatives of different SUMO paralogues demonstrated that xSENP3 shared the same enzymatic specificity as mammalian SENP3 (Fig. S2 D).

We observed a protein that strongly and specifically coprecipitated with xSENP3, which mass spectrometric analysis revealed to be the *Xenopus* homologue of B23/nucleophosmin (xB23/nucleophosmin). We confirmed this interaction by Western blotting of anti-xSENP3 immunoprecipitates (Fig. 1 B). Given the low levels of xSENP5 within XEEs, we used an alternative strategy to determine whether SENP5 might likewise

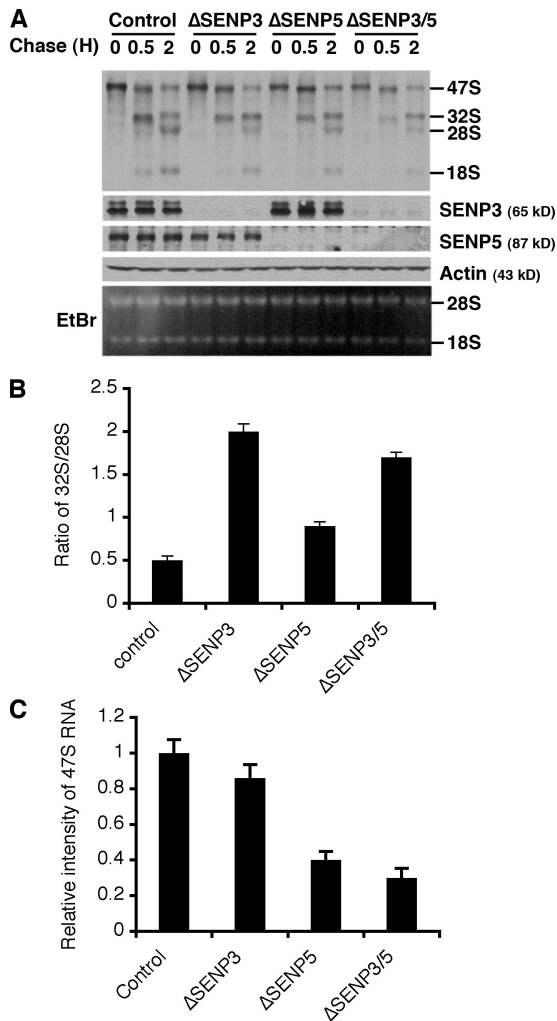


Figure 3. Depletion of SENP3 or SENP5 cause defects in ribosome biogenesis. (A) HeLa cells were transfected with control oligonucleotides (Control) or siRNAs directed against SENP3 (Δ SENP3) and SENP5 (Δ SENP5) or both SENP3 and SENP5 (Δ SENP3/5). 72 h later, the cells were pulsed with [3 H]uridine for 25 min, followed by washing and incubation with fresh media supplemented with 1 mg/ml of cold uridine for the indicated times (in hours). At each time point, equal numbers of cells were harvested for analysis of rRNA synthesis and processing. (Bottom) Western blots of cell extracts to monitor SENP3 and SENP5 and Western blotting of actin as a loading control. Ethidium bromide staining shows the amount of total RNA loaded in each lane. (B) The amounts of 28S and 32S RNAs were quantitated within three independent experiments as in A after 2 h. Ratios of 32S to 28S RNAs were calculated for each experiment. Bars represent the mean values calculated from the three experiments \pm SD. (C) The amount of 47S pre-rRNA transcript was quantitated at the initiation of the chase period (0 h) within three independent experiments as in A and normalized to the levels found in cells treated with control oligonucleotides. Bars represent the mean of normalized values from the three experiments \pm SD.

associate with xB23/nucleophosmin. FLAG-tagged xSENP5 was translated within XEEs (Boyarchuk et al., 2007), followed by precipitation with anti-FLAG or anti-xB23/nucleophosmin antibodies. Like xSENP3, we found that FLAG-tagged xSENP5 strongly bound with xB23/nucleophosmin in XEEs (Fig. 1 B).

Mammalian cells lacking B23/nucleophosmin show defects in ribosome biogenesis and particularly in 32S to 28S RNA processing (Itahana et al., 2003). The association of B23/nucleophosmin and nucleolar SENPs, as well as their colocaliza-

tion and phenotypic similarities, lead us to further examine their relationship. Both SENP3 and SENP5 levels decreased dramatically after RNAi-mediated depletion of B23/nucleophosmin (Fig. 4). This could be observed either by immunoblotting (Fig. 4 A) or by examination of GFP fluorescence in U2OS cells stably expressing GFP-SENP3 or GFP-SENP5 (Fig. 4 B). SENP1 and SENP2 levels did not change after B23/nucleophosmin depletion (Fig. 4 A). As in experiments where SENP3 and SENP5 were codepleted (Fig. 2), depletion of B23/nucleophosmin caused a shift of SUMO protein distribution toward nucleoli (Fig. 4 C). Our findings suggest that B23/nucleophosmin physically interacts with SENP3 and SENP5 and regulates their abundance and that it thus plays a critical role in controlling the profile of SUMO conjugates within nucleoli through SENP3 and SENP5.

Several observations indicated that SENP3 and SENP5 loss was caused by increased degradation rather than decreased expression. First, GFP-SENP3 and GFP-SENP5 were not transcribed from the native SENP3 and SENP5 promoters, so the drop in their levels upon B23/nucleophosmin depletion (Fig. 4 B) argues that repression of those promoters cannot account for changes in protein levels. Second, the concentrations of SENP3 and SENP5 mRNAs were not substantially altered by B23/nucleophosmin depletion in HeLa cells, as measured by RT-PCR (unpublished data), further arguing against B23/nucleophosmin control of SENP3 and SENP5 transcription or mRNA stability. Third, B23/nucleophosmin-depleted cells did not show a substantial drop in overall protein translation, as measured by incorporation of [35 S]methionine (unpublished data), indicating that preexisting ribosomes were largely sufficient to maintain protein synthesis levels. Notably, depletion of a key ribosomal assembly factor, Rrp9 (Venema et al., 2000), did not destabilize SENP3 and SENP5 or cause substantial nucleolar accumulation of SUMO proteins (unpublished data), demonstrating that their loss was not a simple consequence of ribosome synthesis inhibition but may be more specifically linked to the function of B23/nucleophosmin.

Finally, SENP3 and SENP5 levels in B23/nucleophosmin-depleted cells showed substantial, albeit incomplete, recovery upon treatment with the proteasome inhibitor MG132, which is consistent with the notion that they are subject to degradation in the absence of B23/nucleophosmin (Fig. 4 D). Stable cell lines expressing GFP-SENP3 and SENP5 showed a partial redistribution of GFP signals after B23/nucleophosmin depletion and MG132 treatment, with an increase in the ratio of nucleoplasmic to nucleolar distribution of both fusion proteins (unpublished data). This observation might indicate a role for B23/nucleophosmin in retention of these Ulp/SENPs within the nucleolus. However, we noted that the distribution of many other nucleolar proteins was rearranged after MG132 treatment, so it is also possible that relocalization of GFP-SENP3 and GFP-SENP5 may reflect alterations of nucleolar structure.

We hypothesized that failure to deconjugate some SUMO species might disrupt ribosome biogenesis in the absence of SENP3 and SENP5. We therefore examined the SUMOylation of mammalian homologues of ribosomal proteins or ribosome assembly factors that have been implicated as SUMO conjugation targets in yeast (Panse et al., 2004, 2006; Wohlschlegel

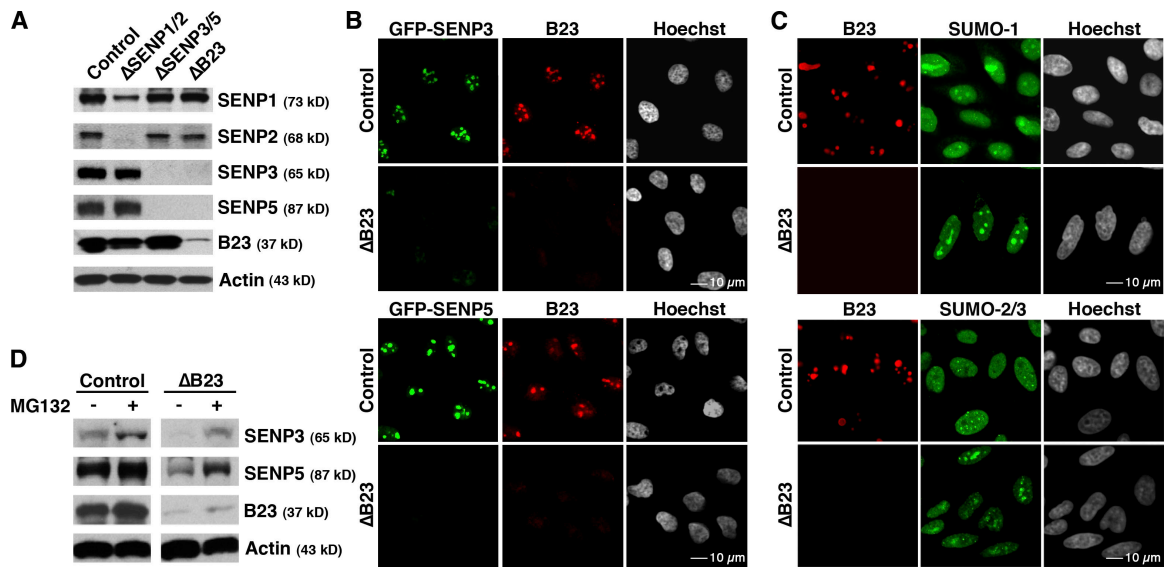


Figure 4. B23/nucleophosmin regulates SENP3 and SENP5 abundance. (A) HeLa cells were transfected with control oligonucleotides (left lane), siRNAs for codepletion of SENP1 and SENP2 (second lane), siRNAs for codepletion of SENP3 and SENP5 (third lane), or siRNAs for depletion of B23/nucleophosmin (right lane). After 72 h, the cells were harvested and immunoblotted with the indicated antibodies, where actin serves as a loading control. (B) U2OS cells stably expressing either GFP-SENP3 (top) or GFP-SENP5 (bottom) were transfected with control or B23/nucleophosmin siRNA, as indicated. After 72 h, the cells were washed and fixed with 4% paraformaldehyde and stained with antibodies against B23/nucleophosmin (red). Signals from the GFP-SENP3 and GFP-SENP5 fusion proteins are shown in green. (C) As in A, HeLa cells were transfected with control oligonucleotides or with siRNAs for depletion of B23/nucleophosmin. After 72 h, the cells were stained with antibodies against B23/nucleophosmin (red) and against either SUMO-1 or SUMO-2/3 (green), as indicated. (D) 48 h after transfection with control or B23/nucleophosmin siRNAs, HeLa cells were treated for 6 h with 20 μ M of proteasome inhibitor MG132 (+) or DMSO (-). The cells were harvested and subjected to Western blotting analysis with antibodies against SENP3, SENP5, B23/nucleophosmin, and actin, as indicated.

et al., 2004; Denison et al., 2005; Hannich et al., 2005). Using cells that stably expressed His₆-tagged SUMO-1 (His-SUMO1F) or SUMO-2 (His-SUMO2F) proproteins, we examined changes in electrophoretic mobility of potential conjugation targets by Western blotting after codepletion of SENP3 and SENP5. We also purified the SUMO-conjugated fraction from each cell line by affinity chromatography and examined whether SUMOylated forms of the proteins could be found by Western analysis.

A subset of proteins showed clearly altered SUMOylation patterns under these circumstances: GNL2, the mammalian homologue of a 60S preribosomal export factor, showed a supershifted form upon depletion of SENP3/5 (Fig. 5), which was verified as a SUMOylated form through its preferential retention on nickel–nitrilotriacetic acid (Ni-NTA) agarose beads. We observed a supershifted form of the 60S ribosomal subunit RPL37A that was retained on Ni-NTA agarose beads in the absence of SENP3/5 (Fig. 5, top), suggesting that it was likewise subject to enhanced modification. Other nucleolar proteins (fibrillarin, DDX3, DDX17, and NVL2; unpublished data) did not show evidence of SUMOylation in this assay. Although this is an incomplete survey of potential conjugation targets within the 60S ribosomal biogenesis pathway, it demonstrates that multiple pathway components are SUMOylation targets, as in yeast. More importantly, enhanced RPL37A and GNL2 SUMOylation after depletion of SENP3 and SENP5 implicates these proteases in the control of ribosome biogenesis through this modification.

While this manuscript was under revision, Haindl et al. (2008) reported that SENP3 and B23/nucleophosmin physically interact and that loss of SENP3 disrupts rRNA processing. They

argued that SENP3 acts upstream of B23/nucleophosmin, causing inhibition of ribosome biogenesis through increased B23/nucleophosmin SUMOylation. In our hands, depletion of SENP3 and SENP5 by RNAi, either singly (not depicted) or in combination (Fig. 5), did not cause a substantial SUMOylation of B23/nucleophosmin. We do not know why our results differ from those of

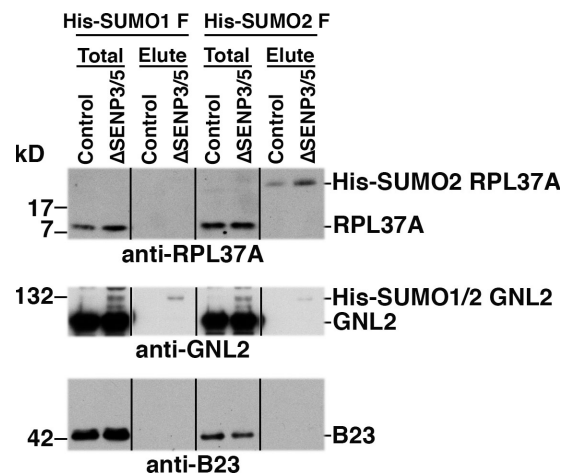


Figure 5. Enhanced SUMO modification of RPL37A and GNL2 after depletion of SENP3 and SENP5. U2OS stably expressing full-length His-tagged versions of SUMO-1 and SUMO-2 (His-SUMO1F and His-SUMO2F) were transfected with siRNAs for codepletion of SENP3 and SENP5 or with control oligonucleotides. After 72 h, the cells were harvested and His₆-SUMO-modified proteins were isolated. Total cell extracts and His₆ affinity fractions were analyzed by Western blotting with antibodies against RPL37A (top), GNL2 (middle), or B23/nucleophosmin (bottom).

Haindl et al. (2008), but suspect that the relatively low levels of His-tagged SUMO proteins expressed in our stable cell lines may mimic physiological conditions more closely than conditions of transient expression. In any case, our results do not suggest that B23/nucleophosmin is itself the primary target of SENP3 or SENP5. As an alternative model, we note that B23/nucleophosmin interacts with ribosomes (Grisendi et al., 2006), so that it might act as an adaptor for targeting of SUMO proteases to ribosomal proteins. Consistent with this idea, 60S ribosomal components Rpl26 and RplP0 are coprecipitated from XEEs with xSENP3 in a xB23/nucleophosmin-dependent manner (Fig. 1 C).

The requirement for B23/nucleophosmin in ribosome synthesis has been proposed to include both action as an endonuclease (Savkur and Olson, 1998) and as a chaperone (Szebeni and Olson, 1999). Our data show that regulation of SUMOylation through SENP3 and SENP5 is another major aspect of B23/nucleophosmin function in this process. The capacity of xB23/nucleophosmin to link xSENP3 with ribosomes suggests that it may recruit SUMO proteases to maturing ribosomal particles. Interestingly, B23/nucleophosmin has been implicated in a variety of apparently unrelated cellular processes (Grisendi et al., 2006), many of which are also dependent on the SUMO conjugation (Hay, 2005). We therefore speculate that altered SUMOylation may be a simple, unifying mechanism that underlies much of the apparent plurality of B23/nucleophosmin functions.

Materials and methods

Chemicals and reagents

Human testis QUICK-Clone cDNA, human multiple tissue cDNAs, pEGFP, and pDsRed were obtained from Clontech Laboratories, Inc. Oligofectamine, Rabbit IgG tricolor labeling kit, and geneticin were obtained from Invitrogen. siRNA oligonucleotides (SENP1, AATCCTCCTCAGACAGTTT; SENP2, AACATGCTGAAACTGGGTAAT; SENP3, AAATCCGTACCAAGGGTAT; SENP5, AAGTCCACTGGTCTCTCATT; control, AACTGTCAGTCAGTCGTAGTA), Ni-NTA agarose, and Effectene were obtained from QIAGEN. NHS-Sepharose, protein A-Sepharose, and HRP-conjugated secondary antibody were obtained from GE Healthcare. Mouse monoclonal anti-B23/nucleophosmin and anti-UBF antibodies were from Santa Cruz Biotechnology, Inc. Mouse monoclonal anti-GFP (JL-8) and rabbit anti-GFP (A.v) antibodies were obtained from BD and were used for Western blotting and immunoprecipitation, respectively. Mouse monoclonal anti-actin antibodies were obtained from Sigma-Aldrich. Rabbit anti-RPL37A and anti-GNL2 antibodies were obtained from Abnova. Rabbit anti-NVL antibodies were obtained from Proteintech Group, Inc. Rabbit polyclonal antibodies against Rpl26 and RplP0 were purchased from Bethyl Laboratories, Inc. and Proteintech Group, Inc., respectively. Rabbit antibodies against SUMO-1 and SUMO-2/3 were as described previously (Azuma et al., 2003). Other reagents were obtained from Sigma-Aldrich unless otherwise stated.

cDNA constructs

Human SENP3 and SENP5 complete coding sequences were amplified from a testis cDNA library and subcloned into the XhoI-KpnI or HindIII-BamHI sites of pEGFP-C3, respectively. Full-length human fibrillarin and B23/nucleophosmin cDNAs were amplified from a testis cDNA library and subcloned into the Sall-BamHI and XhoI-HindIII sites of pCMVDSRed-Express vector, respectively. Full-length xSENP3 cDNA was obtained from American Type Culture Collection (IMAGE: 5155254). A full-length xSENP5 cDNA was amplified from a tadpole cDNA library and subcloned into the XhoI-SpeI sites of pT7-FLAG-TR α (a gift of Y.-B. Shi, National Institutes of Health, Bethesda, MD). This construct (pT7-FLAG-TR α -XSENP5) was used for FLAG-tagged xSENP5 expression.

Antibodies and immunological methods

Human SENP3 (amino acids 204–406) and SENP5 (amino acids 1–237) fragments were subcloned into the BamHI-XhoI sites and BamHI-Sall sites

of pET-30a vector, respectively. xSENP3 (amino acids 327–615) and the complete coding sequence of xB23/nucleophosmin were subcloned into the BamHI-Sall sites of pET28a. Recombinant fusions encoded by these cDNAs were expressed in *Escherichia coli* (BL21 [DE3]) and purified over Ni-NTA agarose beads. Polyclonal antibodies against human SENP3 and SEN5 and against xSENP3 were generated in rabbits (Covance). Anti-xB23/nucleophosmin antibodies were generated in rabbits (Pacific Immunology). In all cases, antisera were purified using antigens coupled to NHS-activated Sepharose 4 Fast Flow beads (GE Healthcare).

Cell culture, stable cell lines, and siRNA treatment

HeLa and U2OS cells were grown at 37°C, in a humidified atmosphere of 5% CO₂ in DME supplemented with 2 mM glutamine, 10% fetal bovine serum, and antibiotics. U2OS cells were transfected with plasmids for GFP-SENP3 or GFP-SENP5 using Effectene reagent, and stable cell lines were selected and maintained with medium containing 0.5 mg/ml geneticin. siRNAs were transfected into HeLa cells using Oligofectamine.

Detection of SUMO-modified substrates

Analysis of SUMOylated substrates (Fig. 5) was performed as described previously (Rodriguez et al., 1999). In brief, U2OS-derived cells stably expressing His₆-tagged full-length SUMO-1 (His-SUMO1F) or SUMO-2 (His-SUMO2F) were depleted of SENP3 and SENP5 by siRNA. 72 h later, the cells were harvested, lysed in lysis buffer (6 M guanidine-HCl, 0.1 M Na₂HPO₄/NaH₂PO₄, 0.01 M Tris-HCl, pH. 8.0, and 10 mM β -mercaptoethanol) plus 5 mM imidazole. After sonication, total cell lysates were mixed with 50 μ l of (Ni-NTA) agarose beads and incubated for 2 h at 23°C. The beads were washed with lysis buffer, followed by buffer A (8 M Urea, 0.1 M Na₂HPO₄/NaH₂PO₄, 0.01 M Tris-HCl, pH. 8.0, 10 mM β -mercaptoethanol, and 0.2% Triton X-100). After washing, the beads were eluted with 200 mM imidazole in 5% SDS, 0.15 M Tris-HCl, pH 6.7, 30% glycerol, and 0.72 M β -mercaptoethanol. The eluted fraction was subjected to SDS-PAGE and Western blotting with anti-RPA37A, -GNL2, or -B23/nucleophosmin antibodies.

Interactions of B23/nucleophosmin with SENP3 or SENP5

Interphase XEEs were prepared as described previously (Orjalo et al., 2006). For Fig. 1 B (top), anti-xSENP3 and -xB23 antibodies or rabbit IgG were conjugated to protein A Dynabeads (Invitrogen). The XEE was supplemented with 10 μ g/ml each of leupeptin, pepstatin, and chymostatin and with 20 μ M Ran-Q69L (Orjalo et al., 2006) and incubated with antibody-coated beads for 1 h at 23°C. The beads were washed with buffer A (250 mM sucrose, 2.5 mM MgCl₂, 1 mM DTT, 100 mM KCl, and 10 mM Hepes, pH 7.7) plus 0.00001% digitonin and protease inhibitors and eluted with 25 μ l of 0.1 M glycine, pH 2.3. For Fig. 1 B (bottom), pT7-FLAG-TR α -xSENP5 mRNA was made using an mMessage mACHINE T7 kit (Applied Biosystems) and translated in XEEs (Boyarchuk et al., 2007). 25 μ l of the reaction was mixed with 25 μ l of interphase XEE and 20 μ M Ran-Q69L. The mixture was diluted 10-fold with buffer B (250 mM sucrose, 2.5 mM MgCl₂, 1 mM DTT, 50 mM KCl, 100 mM Hepes, pH 7.7, and 0.00001% digitonin) and clarified by centrifugation. Mouse anti-FLAG antibody (M2; Sigma-Aldrich), rabbit anti-xB23, nonspecific mouse IgG, or nonspecific rabbit IgG were added to aliquots of the clarified supernatant and incubated for 1 h on ice before addition of 15 μ l of preblocked protein G-Sepharose (GE Healthcare). After 1 h at 4°C with rotation, the beads were pelleted, washed with buffer A plus 0.00001% digitonin, and eluted with 25 μ l of 0.1 M glycine, pH 2.3.

In Fig. 1 C, interphase XEEs were depleted using protein A Dynabeads coupled with anti-xB23/nucleophosmin antibodies or mock treated with rabbit IgG-coupled control beads. Resultant XEEs were supplemented with protease inhibitors and 20 μ M Ran-Q69L, and immunoprecipitations with anti-xSENP3 antibody or rabbit IgG were performed as described in the previous paragraph. Bound proteins were eluted with 0.1 M glycine, pH 2.3.

In all cases, equal elution volumes were subjected to SDS-PAGE and Western blotting. In Fig. 1, protein A-HRP was used for visualization of xSENP3. Anti-mouse IgG-HRP was used for FLAG epitope visualization. Anti-rabbit HRP was used for visualization of all other antibodies.

Immunofluorescence microscopy and Western blotting

Cells were grown on LabTeckll coverslip-bottomed chambers or glass slide coverslips. 72 h after transfection with siRNAs, cells were fixed for 5 min with 4% formaldehyde in PBS and permeabilized for 5 min with 0.5% Triton X-100 in PBS. The cells were blocked for 1 h in PBS containing 1% bovine serum albumin. After washing with PBS, the cells were incubated with primary antibodies diluted 1:200 in blocking solution for 1 h. The coverslips were washed and incubated for 1 h with AlexaFluor 488-conjugated

goat anti-rabbit or AlexaFluor 568-conjugated goat anti-mouse secondary antibodies (Invitrogen) diluted 1:500 in blocking solution. All the incubations were performed at 23°C. After antibody incubations, the cells were washed twice with PBS and Hoechst 33258 was added to the final washing solution for 1 min to stain the DNA. Coverslips were mounted in Vectashield (Vector Laboratories). Fluorescence images were captured using a confocal microscope (LSM510 META; Carl Zeiss, Inc.) equipped with a 40x Plan Neofluar objective, with confocal microscopy software (SP2 version 3.2; Carl Zeiss, Inc.). Images were analyzed using Photoshop 7.0 (Adobe). Western blotting was performed using standard protocols (Gallagher et al., 1998). Unless otherwise indicated, all antibodies were used at a dilution of 1:2,000 for Western blotting. Electrophoretic migration of bands in all Western blots are indicated with respect to molecular mass standards run on the same SDS-PAGE gels.

Metabolic labeling and analysis of [³H]uridine-labeled RNA

72 h after transfection with SENP3 or SENP5 siRNAs, HeLa cells were pulsed in DME containing [³H]uridine (10 µCi/ml) for 25 min, and then chased in nonradioactive media for the indicated times in the presence of 1 mg/ml of cold uridine (EMD). At each point, the same number of cells was harvested. Total RNA was extracted with Trizol reagent (Invitrogen) and suspended with diethylpyrocarbonate-treated water. Formaldehyde loading dye (Applied Biosystems) was added before heat treatment at 65°C for 45 min. RNAs were separated on a 1% agarose-denaturing gel containing 0.55 M formaldehyde. Formaldehyde was removed by washing with water for 40 min, and the gel was treated with 7.5 mM NaOH to hydrolyze the RNA. After soaking the gel within 20x SSC buffer for 45 min, the RNA was transferred to a nylon membrane (GE Healthcare) overnight. After transfer, RNA was cross-linked to the membrane with UV light. The membrane was dried, sprayed by EN³HANCE (PerkinElmer), and exposed to BioMax XAR film (Kodak) at -80°C.

Online supplemental material

Fig. S1 shows the quantitation of SUMO redistribution after SENP3, SENP5, and B23/nucleophosmin depletion. Fig. S2 shows SENP3 and SENP5 paralogue preferences and expression patterns. Fig. S3 shows mislocalization of ribosomal processing factor NVL2 in the absence of SENP3 and SENP5. Online supplemental material is available at <http://www.jcb.org/cgi/content/full/jcb.200807185/DC1>.

We would like to thank Dr. Hyunja Nam for help in optimizing siRNA depletions.

This work was supported by National Institute of Child Health and Human Development intramural funds (to C. Yun, Y. Wang, D. Mukhopadhyay, P. Backlund, A. Yergay, and M. Dasso) and by National Institutes of Health grant #5R01GM066355 (to N. Kalli and K.D. Wilkinson).

Submitted: 30 July 2008

Accepted: 20 October 2008

References

Ayaydin, F., and M. Dasso. 2004. Distinct in vivo dynamics of vertebrate SUMO paralogues. *Mol. Biol. Cell.* 15:5208–5218.

Azuma, Y., A. Arnaoutov, and M. Dasso. 2003. SUMO-2/3 regulates topoisomerase II in mitosis. *J. Cell Biol.* 163:477–487.

Boisvert, F.M., S. van Koningsbruggen, J. Navascues, and A.I. Lamond. 2007. The multifunctional nucleolus. *Nat. Rev. Mol. Cell Biol.* 8:574–585.

Boyarchuk, Y., A. Salic, M. Dasso, and A. Arnaoutov. 2007. Bub1 is essential for assembly of the functional inner centromere. *J. Cell Biol.* 176:919–928.

Denison, C., A.D. Rudner, S.A. Gerber, C.E. Bakalarski, D. Moazed, and S.P. Gygi. 2005. A proteomic strategy for gaining insights into protein sumoylation in yeast. *Mol. Cell. Proteomics.* 4:246–254.

Di Bacco, A., J. Ouyang, H.Y. Lee, A. Catic, H. Ploegh, and G. Gill. 2006. The SUMO-specific protease SENP5 is required for cell division. *Mol. Cell. Biol.* 26:4489–4498.

Gallagher, S.R., S.E. Winston, S.A. Fuller, and J.G.R. Hurrell. 1998. Immunoblotting and immunodetection. In *Current Protocols in Cell Biology*. J.S. Bonifacino, M. Dasso, J. Lippincott-Schwartz, J.B. Harford, and K.M. Yamada, editors. John Wiley & Sons, Inc., New York. 6.2.1–6.2.20.

Gong, L., and E.T. Yeh. 2006. Characterization of a family of nucleolar SUMO-specific proteases with preference for SUMO-2 or SUMO-3. *J. Biol. Chem.* 281:15869–15877.

Grisendi, S., C. Mecucci, B. Falini, and P.P. Pandolfi. 2006. Nucleophosmin and cancer. *Nat. Rev. Cancer.* 6:493–505.

Haindl, M., T. Harasim, D. Eick, and S. Muller. 2008. The nucleolar SUMO-specific protease SENP3 reverses SUMO modification of nucleophosmin and is required for rRNA processing. *EMBO Rep.* 9:273–279.

Hannich, J.T., A. Lewis, M.B. Kroetz, S.J. Li, H. Heide, A. Emili, and M. Hochstrasser. 2005. Defining the SUMO-modified proteome by multiple approaches in *Saccharomyces cerevisiae*. *J. Biol. Chem.* 280:4102–4110.

Hay, R.T. 2005. SUMO: a history of modification. *Mol. Cell.* 18:1–12.

Hay, R.T. 2007. SUMO-specific proteases: a twist in the tail. *Trends Cell Biol.* 17:370–376.

Itahana, K., K.P. Bhat, A. Jin, Y. Itahana, D. Hawke, R. Kobayashi, and Y. Zhang. 2003. Tumor suppressor ARF degrades B23, a nucleolar protein involved in ribosome biogenesis and cell proliferation. *Mol. Cell.* 12:1151–1164.

Johnson, E.S. 2004. Protein modification by SUMO. *Annu. Rev. Biochem.* 73:355–382.

Li, S.J., and M. Hochstrasser. 1999. A new protease required for cell-cycle progression in yeast. *Nature.* 398:246–251.

Li, S.J., and M. Hochstrasser. 2000. The yeast ULP2 (SMT4) gene encodes a novel protease specific for the ubiquitin-like Smt3 protein. *Mol. Cell. Biol.* 20:2367–2377.

Liu, X., Z. Liu, S.W. Jang, Z. Ma, K. Shinmura, S. Kang, S. Dong, J. Chen, K. Fukasawa, and K. Ye. 2007. Sumoylation of nucleophosmin/B23 regulates its subcellular localization, mediating cell proliferation and survival. *Proc. Natl. Acad. Sci. USA.* 104:9679–9684.

Mukhopadhyay, D., and M. Dasso. 2007. Modification in reverse: the SUMO proteases. *Trends Biochem. Sci.* 32:286–295.

Orjalo, A.V., A. Arnaoutov, Z. Shen, Y. Boyarchuk, S.G. Zeitlin, B. Fontoura, S. Briggs, M. Dasso, and D.J. Forbes. 2006. The Nup107-160 nucleoporin complex is required for correct bipolar spindle assembly. *Mol. Biol. Cell.* 17:3806–3818.

Panse, V.G., U. Hardeland, T. Werner, B. Kuster, and E. Hurt. 2004. A proteome-wide approach identifies sumoylated substrate proteins in yeast. *J. Biol. Chem.* 279:41346–41351.

Panse, V.G., D. Kressler, A. Pauli, E. Petfalski, M. Gnadig, D. Tollervy, and E. Hurt. 2006. Formation and nuclear export of preribosomes are functionally linked to the small-ubiquitin-related modifier pathway. *Traffic.* 7:1311–1321.

Powers, M., E.K. Evans, J. Yang, and S. Kornbluth. 2001. Preparation and use of interphase *Xenopus* egg extracts. In *Current Protocols in Cell Biology*. J. S. Bonifacino, M. Dasso, J. Lippincott-Schwartz, J.B. Harford, and K.M. Yamada, editors. John Wiley & Sons, Inc., New York. 11.10.1–11.10.24.

Rodriguez, M.S., J.M. Desterro, S. Lain, C.A. Midgley, D.P. Lane, and R.T. Hay. 1999. SUMO-1 modification activates the transcriptional response of p53. *EMBO J.* 18:6455–6461.

Savkur, R.S., and M.O. Olson. 1998. Preferential cleavage in pre-ribosomal RNA by protein B23 endoribonuclease. *Nucleic Acids Res.* 26:4508–4515.

Sherr, C.J. 2006. Divorcing ARF and p53: an unsettled case. *Nat. Rev. Cancer.* 6:663–673.

Szebeni, A., and M.O. Olson. 1999. Nucleolar protein B23 has molecular chaperone activities. *Protein Sci.* 8:905–912.

Venema, J., H.R. Vos, A.W. Faber, W.J. van Venrooij, and H.A. Raue. 2000. Yeast Rrp9p is an evolutionarily conserved U3 snoRNP protein essential for early pre-rRNA processing cleavages and requires box C for its association. *RNA.* 6:1660–1671.

Wohlschlegel, J.A., E.S. Johnson, S.I. Reed, and J.R. Yates III. 2004. Global analysis of protein sumoylation in *Saccharomyces cerevisiae*. *J. Biol. Chem.* 279:45662–45668.